

From two to three-dimensional visualisation of structures in light and confocal microscopy – applications for biomedical studies

Elżbieta Kaczmarek, Rafał Strzelczyk

Laboratory of Morphometry and Medical Image Processing, Chair of Pathology, University of Medical Sciences in Poznań, Przybyszewskiego 49, Poznań, Poland

The aim of this chapter is to show some applications of biomedical image analysis in light and confocal microscopy. First, conventional two dimensional techniques are introduced. Then, spatial visualisation of 2D images extended to 3D space is provided for conventional light microscopy observations of immunohistochemical reactions. Quantification of the expression of colour reactions in histological specimens is also presented. Next, 3D reconstruction and modelling of vascular networks based on confocal microscopy images is presented.

Keywords: spatial visualisation, reconstruction, image analysis, computer-assisted microscopy, confocal microscopy, microvessels, immunohistochemistry

Introduction

Digital image processing and visualisation techniques make a potential benefit in quantitative analysis of image data. Computerized image analysis systems used for analysis of histological or cytological specimens allow us to get quantitative measurements from planar images. The progress of newer microscopical techniques, including confocal microscopy, has led to 3D datasets available by acquiring series of optical images with synchronous image registration on a computer [16].

The aim of this publication is to present potential for biomedical applications of 2D image analysis and 3D visualisation with quantitative analysis of structures in computer assisted microscopy.

Conventional analysis of 2D images

Upon analysis of histological specimens, a quantitative evaluation of microscopy images is associated with a segmentation of investigated structures, for instance cell nuclei, profiles of microvessels, interstitial fibrosis [7, 12] area of demineralization in dental enamel [9], specific colours representing the expression of an immunohistochemical reaction in raw images [2, 3], etc. An example of segmented endothelial cell marker CD34 in human kidney presents Fig. 1. Routinely structures of interest are segmented by thresholding in images converted to greyscale or by colour sampling from raw colour images filtered, if necessary, to reduce noise (Fig. 2). In this example, sampling of colours gave worse result of α -smooth muscle actin segmentation than the segmentation by thresholding. It has to be mentioned, that the use of “eye dropper tool” in image analysis programs can lead to biased segmentation of several objects and often requires repeated tryouts to assure appropriate results.

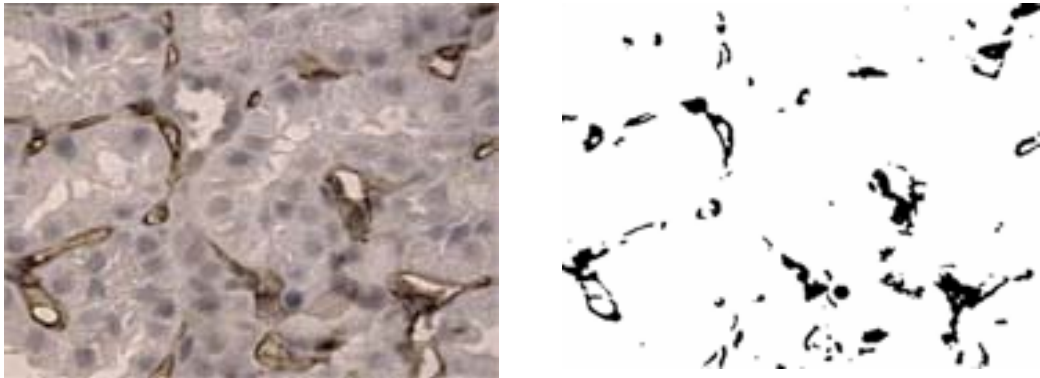


Fig. 1. An image of endothelial CD34 marker in human kidney (left) and its binary representation after segmentation by thresholding (right).

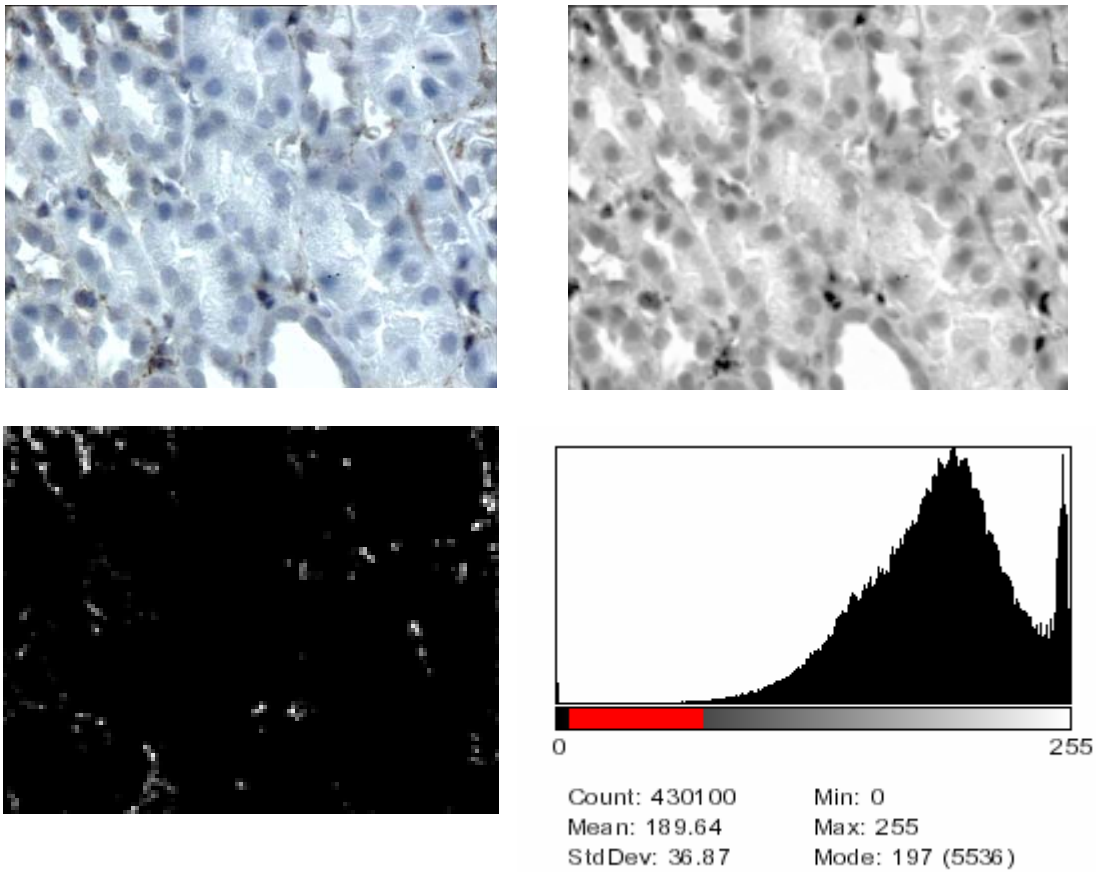


Fig. 2. Segmentation of α -smooth muscle actin in human kidney specimen; raw image (top left); ASMA (black spots) segmented by thresholding (top right); α -smooth muscle actin segmented with "eye dropper" (bottom left); histogram of grey levels for thresholding of colours from 7 to 72 in the greyscale image (bottom right).

Wrongly segmented objects should be then removed, often manually. On the other hand, when image brightness distribution is heterogeneous, the segmentation by thresholding can determine too low quantity of analysed structures or extracts additional objects to structures of interest.

Therefore, we decided to introduce a technique based on a spatial representation of objects of interest [11].

3D visualisation of structures subjected to segmentation

To avoid difficulties related with heterogeneous image brightness in HSB colour space, we decided to expand 2D images into 3D space by introducing brightness as the third dimension and a triangulation of 3D bars (representing colour brightness) as in finite element theory. In this way, objects extended into 3D space were represented in forms of solid figures combined with prisms and pyramids (Fig 3.).

To improve a visibility of objects of interest, the scenery behind the objects was reduced to a background with the use of three filters.

At first, a filter of brightness extracted objects having brightness (as the third dimension) greater than an assumed threshold value. The remaining elements were settled to the lowest value resulting in a horizontal plane.

Second, a colour filtering, based on HSB colour system, allowed us to extract the objects in the colour of interest (i.e. a colour marker of a reaction performed in a histological specimen).

Third, a filter of saturation removed background in colour images. The filters were calibrated for each series of images representing a specimen.

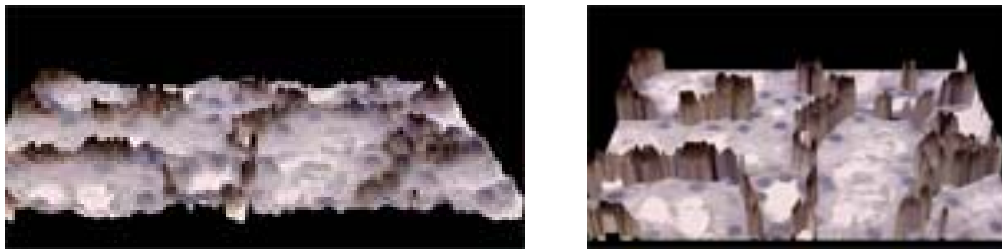


Fig 3. An example of 3D visualisation of an image with CD34+ in human kidney (left); the scenery behind CD34+ reduced to a horizontal plane represents the expression of the endothelial marker CD34 (right).

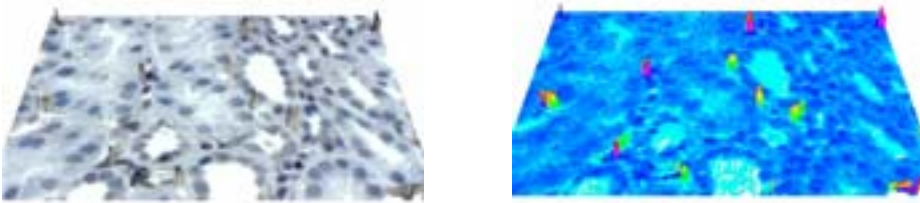


Fig 4. An example of 3D visualisation of an image with α -smooth muscle actin in human kidney (left); and its conversion to 256 colours (right).

An example of α -smooth muscle actin segmentation by using its 3D is presented in Fig. 4.

To make the quantification of α -smooth muscle actin easier, the image in original colours was converted to reduced scale of 256 colours. This technique is particularly useful for analysis of clustered small spots of selected colours representing investigated objects in digital images.

Quantification of the expression of a colour reaction

To measure colour specific structures in raw histological images their area can be determined based on the total number of pixels belonging to the segmented objects and related to the reference area giving the result of area fraction. In 3D images, surface and volume was also determined on the basis of the total number of pixels belonging to the segmented solid objects combined from prisms and pyramids. Assuming that the maximum intensity of colour of the reaction cannot exceed 255 and the thickness of all histological sections is the same, the expression of a reaction REXP was assessed as the ratio $REXP = V / 255$.

3D reconstruction of vascular networks

Serial sectioning combined with three-dimensional reconstruction was used to help researcher understand the structure of individual organs, tissues and cells, and study the relationships and connections between them. In 19th century, His [4], the pioneer of three-dimensional (3D) reconstructions, used two-dimensional (2D) serial sections to produce precise 3D models of embryos. The mechanisms of angiogenesis (blood vessels growth and formation) were also studied by means of 3D models, in particular, renal capillaries. The concepts that glomerular capillaries form a network was first published by Boyer [1] who created a beautiful model of a human glomerulus reconstructed in plastic from 2 micron thick paraffin serial sections, unfortunately no quantitative data were derived from this model. Beginning after, vascular networks of various complexities have been reconstructed in humans and animals, for examples human cornea [20], renal glomeruli [18, 19, 21], abdominal mesentery [10]. Vascular networks can be described by their length and topological properties such as the number of capillaries, bifurcation points related with the branching process and formation of lobules [15, 18, 19].

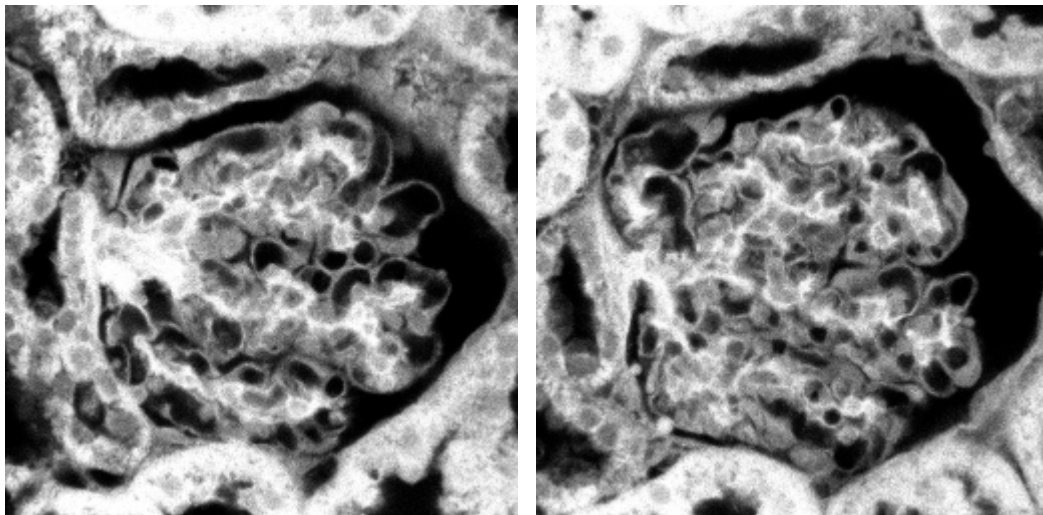


Fig. 5. Examples of epifluorescent images of renal glomeruli (10 microns apart) acquired from a confocal microscope.

However techniques of 3D reconstructions based on serial sections caused several difficulties.

Shifting or rotating each image to align profiles of vessels segmented in two consecutive sections often alters the reconstruction. Profiles of reconstructed structures (for instance capillaries) have to be aligned to each other to reconstruct them.

Avoiding physical distortions of specimens due to cutting and having different alignments from various imaging planes increased the interest in confocal microscopy. For reconstruction of capillary networks, confocal microscopy offers an opportunity to acquire consecutive sections of branching capillaries along the optical axis and analyse them in 3D space (Fig. 5).

Reconstructions of renal glomeruli presented in this chapter were created from at least 100 confocal images (0.5 microns apart) of a normal rat glomerulus. Profiles of capillaries were enhanced by rank filters and segmented by thresholding [7, 8]. Then, capillary networks were reconstructed by stacking up segmented profiles of capillaries (Fig. 6) or by isosurface algorithms [6]. Those models were not particularly useful for assessment of the length of capillaries. Therefore capillary networks were also represented in form of graphs created from edges joining centres of gravity of segmented profiles (Fig. 7). Colours of edges were assigned based on Euclidean distances between connected centres of gravity. All edges forming graph connected component have the same colour.

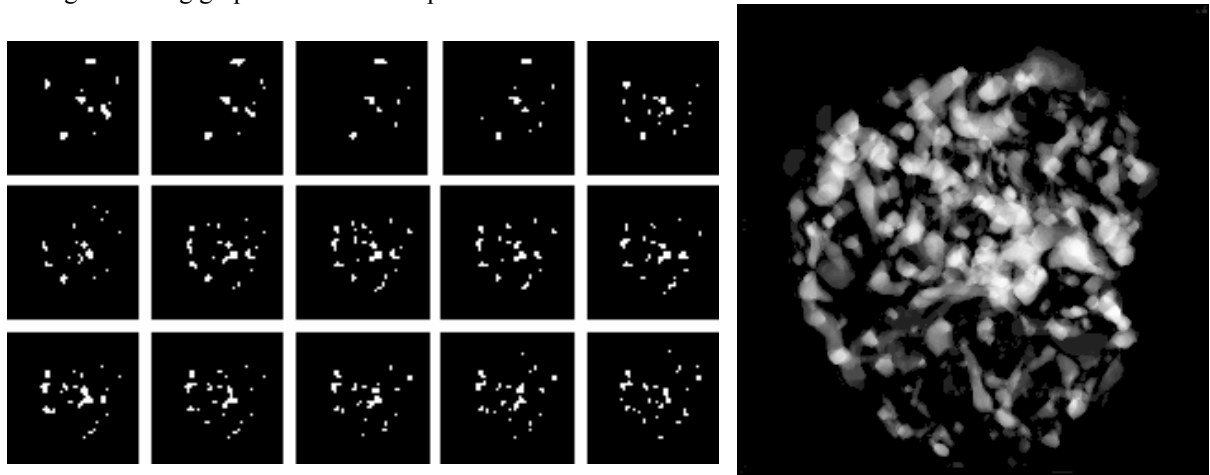


Fig. 6. Fragment of a series of segmented capillary profiles (left) and a 3D network built up from the stack of segmented profiles (right).

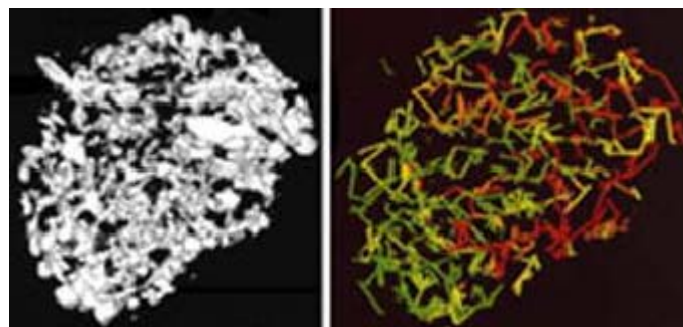


Fig. 7. Model of a glomerular network created from segmented capillary profiles by isosurface algorithm (left) and its graph-theoretical representation (right).

Different connected components that were close together were in similar colours. Graph-theoretical modelling of vascular networks from confocal epifluorescent images made available their 3D reconstruction optimal and quite fast [7, 8].

From graphs representing capillary networks, the total capillary length was estimated. The length of normal rat capillary networks ranged from 3500 to 9500 microns [5, 7, 8].

Vessel architectural complexity can be also visualized with the endothelial marker CD34 [13, 17].

The development of 3D imaging software for confocal microscopy studies enabled also spatial visualisation of CD34 distribution on cord blood and bone marrow [22], however the cost of these studies is rather high.

Final comments

Image analysis methods widely used for semi or fully automatic quantification of a colour reaction in histological images often met segmentation problems. Mathematical morphology operations on the grey level images present several limitations related with various colour intensities of the staining. Therefore, this method can underestimate a quantitative assessment of α -SMA content in renal interstitium. To locate the distribution of α -SMA in renal tissue, spots with positive reaction were counted by computer image analysis program by extracting the single positive cells for creating a combined image by the "adding procedure". The structures of interest were interactively discriminated by the operators using the cursor and then automatically the area was calculated [14]. Their results received in patients with mild (the average 30.1 per 1000 μm^2 of renal interstitium) and moderate histological lesions (the average 40.2 per 1000 μm^2 of renal interstitium) were comparable with our results of cases with moderate changes. Three-dimensional reconstructions of rat renal glomeruli are similar to earlier reconstructions [15, 18, 19].

References

- [1] C.C. Boyer: *The vascular pattern of the renal glomerulus as revealed by plastic reconstruction from serial sections* Anat Rec Vol. 125 (1956), p. 443-441
- [2] R. Brelinska, E. Kaczmarek, D. Ostalska: *Kinetics of thymic stroma development in the foetal period* Folia Histochem Cytobiol Vol. 39 (2001), pp. 195-196.
- [3] R. Brelinska, D. Ostalska, E. Kaczmarek, K. Kowalska: *Stages of the rat thymic medulla development in foetal period*. Folia Histochem Cytobiol Vol. 40 (2002), pp. 171-172.
- [4] W. His: *Anatomie Menschlicher Embryonen* (Leipzig: Vogel, 1880).
- [5] E. Kaczmarek: *Quantification of three-dimensional vascular patterns in renal glomeruli* Acta Stereol Vol. 15 (1996), pp. 103-200.
- [6] E. Kaczmarek: *Visualizing of kidney capillaries with three-dimensional tree structures* Proceedings of 12th Spring Conference on Computer Graphics. Bratislava-Budemrice June 5-7, (Comenius University, Bratislava, Czech Republik 1996, pp. 77-86).
- [7] E. Kaczmarek, R.L. Becker: *Three-Dimensional Modeling of Renal Capillary Networks*. Annal Quant Cytol Histol Vol. 19 (1997), pp. 93-101.
- [8] E. Kaczmarek: *Visualization and modeling of renal capillaries from confocal images*. Med Biol Eng Comput Vol. 37 (1999), pp. 273-277.
- [9] E. Kaczmarek, T. Matthews-Brzozowska, B. Miskowiak: *Digital image analysis in dental research applied for treatment of fissures on occlusal surfaces of premolars*. Annals Biomed Eng Vol. 31 (2003), pp. 931-936.
- [10] K. Ley, A.R. Pries, P. Gaetgens: *Topological structure of rat mesenteric microvascular networks*. Microvasc Res Vol. 32 (1986), pp. 315-332.
- [11] E. Nieruchalska, R. Strzelczyk, A. Wozniak, J. Zurawski, E. Kaczmarek, W. Salwa-Zurawska: *A quantitative analysis of the expression of α -smooth muscle actin in mesangioproliferative (GnMes) glomerulonephritis* Folia Morphol Vol. 62 (2003), pp. 451-453.
- [12] M. Masseroli, F. O'Valle, M. Andujar, C. Ramirez, M. Gomez-Morales, J. De Dios Luna, M. Aguilar, D. Aguilar, M. Rodriguez-Puyol, R.G. Del Moral: *Design and Validation of a New Image*

- Analysis Method for Automatic Quantification of Interstitial Fibrosis and Glomerular Morphometry*. Lab Invest Vol. 78 (1998), pp.511-522.
- [13] K. Okon, A. Szumera, M. Kuzniewski: *Are CD34+ well fund in renal interstitial fibrosis?* Am J Nephrol Vol. 23 (2003), pp. 409-414.
- [14] E. Ranier, L. Gesualdo, G. Grandaliano, E. Maiorano, F.P. Schena: *The role of α -smooth muscle actin and platelet-derived growth factor- β receptor in the progression of renal damage in human IgA nephropathy*. J Nephrol Vol. 14 (2001), pp. 253-262.
- [15] A. Remuzzi, B. Brenner, V. Pata, G. Tebaldi, R. Mariano, A. Belloro, G. Remuzzi: *Three dimensional reconstructed glomerular capillary network: Blood flow distribution and local filtration*. Amer J Physiol Vol. 263 (1992), pp. F562-F572.
- [16] R.A. Robb: *Three-Dimensional Visualization in Medicine and Biology* (In Bankman IN, Editor-in-Chief. Handbook of Medical Imaging. Processing and Analysis. Academic Press, San Diego, 2000, pp. 685-712).
- [17] E. Sabo E, A. Boltenko, Y. Sova, A. Stein, S. Kleinhaus, M.B. Resnick: *Microscopic Analysis and Significance of Vascular Architectural Complexity in Renal Cell Carcinoma*. Clinical Cancer Research Vol. 7 (2001) pp. 535-537.
- [18] SM. Shea: *Glomerular hemodynamics and vasculature structure: The pattern and dimensions of a single rat glomerular capillary network reconstructed from ultrathin sections*. Microvasc Res Vol. 18 (1979) pp. 129-143.
- [19] SM. Shea, J. Raskova: *Glomerular hemodynamics and vasculature structure in uremia: A network analysis of glomerular path length and maximal blood transit times computed for a microvascular model reconstructed from subserial ultrathin sections*. Microvasc Res Vol. 28 (1984) pp. 37-50.
- [20] S. Tong, F. Yuan: *Numerical simulations of angiogenesis in the cornea*. Microvasc Res Vol. 61 (2001) pp. 14-27.
- [21] E.M. Wah, F.H. Daniels, E.F. Leonard, C. Levinthal, S. Cortell: *A graph theory model of the capillary network and its development*. Microvasc Res Vol. 27 (1984) pp. 96-109.
- [22] K.A. Whitting, C.P. McGuckin, Wertheim, D. Pearce, Pettengelr. *Three-dimensional analysis of CD34 sialomucin distribution on cord blood and bone marrow*. Br J Haematol Vol. 122 (2003) pp. 771-777.